Alkyl Side-Chain Length Effects on Fluorescence Dynamics, Lamellar Layer Structures, and Optical Anisotropy of Poly(diphenylacetylene) Derivatives

Giseop Kwak,*,† Masashi Minakuchi,‡ Toshikazu Sakaguchi,§ Toshio Masuda,|| and Michiya Fujiki*,‡

Department of Polymer Science, Kyungpook National University, 1370 Sankyuk-dong, Buk-ku, Daegu 702-701, Korea; Graduate School of Materials Science, Nara Institute of Science and Technology, 8916-5 Takayama, Ikoma, Nara 630-0101, Japan; Department of Materials Science and Engineering, Graduate School of Engineering, University of Fukui, Bunkyo, Fukui 910-8507, Japan; and Department of Polymer Chemistry, Graduate School of Engineering, Kyoto University, Katsura Campus, Kyoto 615-8510, Japan

Received November 21, 2007
Revised Manuscript Received February 4, 2008

Recently, highly efficient and highly polarized fluorescent polymers have attracted much attention due to their potential applications in the fields of display devices, such as organic light-emitting devices (OLED).[1] To develop such advanced fluorescence materials with both a high quantum yield and a highly optical anisotropy, many efforts have been directed toward molecular design and materials processing.

Poly(diphenylacetylene)s are recognized as intensely emissive materials because of effective exciton confinement within the main chain due to the steric hindrance and/or intramolecular electron interactions of bulky aromatic substituents such as phenyl rings.[2] Additionally, poly(diphenylacetylene)s have extremely high molecular weights of $>1.0 \times 10^6$ g/mol by coordination polymerization in the presence of group 5 transition-metal catalysts, and their backbones are expected to adopt a considerably stiff main-chain structure due to bulky phenyl rings with strictly limited rotational freedom.[3] The high molecular weight and the inherent chain stiffness allow for lyotropic liquid crystallinity. Recently, our research group reported lyotropic liquid crystallinity in a poly(diphenylacetylene) bearing an *n*-octadecylsilane moiety in the side chain, poly(1-phenyl-2-*p*-{dimethyl-*n*-octadecylsilylphenyl}acetylene) (**1** in Chart 1).[4] This is the first report of lyotropic liquid crystallinity in a disubstituted acetylene polymer. The polymer had a smectic phase structure in a highly concentrated toluene solution, and its sheared film showed highly polarized absorption and fluorescence in the visible region.

Encouraged by these results, we continued investigation of the fluorescence efficiency and optical anisotropy of other poly(diphenylacetylene) derivatives (**2** and **3** in Chart 1) having *n*-octyldimethylsilane and trimethylsilane moieties, respectively, in the side chain. In this study, we thus focused our interests on the effect of the alkyl group length. Although **2** and **3** have almost the same chemical structures as that of **1**, the slight difference in the alkyl length induces significant changes in fluorescence quantum yield, chain stiffness, and optical order parameter. In this paper, we describe in detail the dynamic fluorescence properties, smectic layer structures, and optical anisotropy of **1**–**3**.

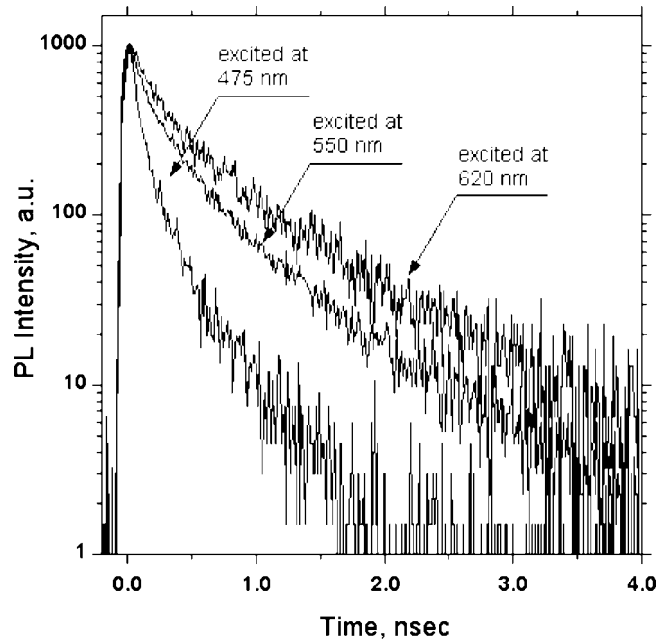

Figure 1. Time-resolved emission decay curve of **1** in cast film at three different emission wavelengths.

The syntheses of **1**–**3** were already reported in previous papers.[3d] The polymers used in this study have high weight-average molecular weights (M_w) of 4.2×10^6, 7.5×10^6, and 5.2×10^6 g/mol, respectively, and polydispersity indices (PDI $= M_w/M_n$) of 2.5, 1.8, and 3.2, respectively.

Polymer **1** showed an endothermic signal around 5 °C in differential scanning calorimetry (DSC) curve, due to a glass transition, whereas the other two polymers, **2** and **3**, containing shorter alkyl groups, did not show apparent transition temperatures.

Conjugating polymers are able to vary their conformation and the effective conjugating sequence length. Accordingly, their electronic states are often widely distributed, leading to the production of plural photoexcited energy trapping sites.[5] Although their photoemission decays may obey multiexponential decay due to the distributions, a time course decay curve analysis using the multiexponential decay functions may help us to understand the excited-state dynamics semiquantitatively. In order to investigate the dynamic fluorescence properties of **1**−**3**,

Chart 1. Chemical Structures of Polymers 1–3

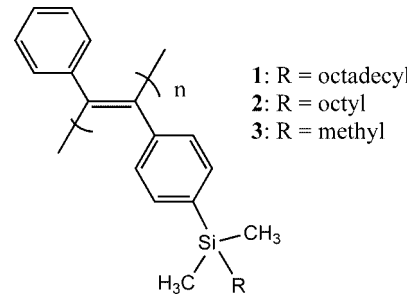

* To whom correspondence should be addressed. E-mail: gkwak@knu.ac.kr (G.K.); fujikim@ms.naist.jp (M.F.).
† Kyungpook National University.
‡ Nara Institute of Science and Technology.
§ University of Fukui.
|| Kyoto University.

10.1021/ma702592u CCC: $40.75
Published on Web 03/07/2008

Table 1. Fluorescence Lifetimes of Polymers 1–3 in Films and Cyclohexane Solutions[a]

		in spin-coated film			in cyclohexane		
polymer	monitor wavelength, nm	τ_1 (f_1), ns	τ_2 (f_2), ns	χ^2	τ_1 (f_1), ns	τ_2 (f_2), ns	χ^2
1	475	0.24 (0.24)	1.18 (0.76)	1.27		1.00 (1.00)	0.72
	550	0.05 (<0.01)	1.43 (>0.99)	1.91		1.11 (1.00)	0.99
	625	0.08 (<0.01)	1.52 (>0.99)	1.37		1.18 (1.00)	0.75
2	475	0.16 (0.66)	0.77 (0.34)	1.27	0.03 (<0.01)	0.76 (>0.99)	1.84
	550	0.03 (<0.01)	1.07 (>0.99)	1.37	0.01 (<0.01)	0.85 (>0.99)	1.07
	625	0.05 (<0.01)	1.23 (>0.99)	0.80	0.09 (<0.01)	0.92 (>0.99)	0.79
3	475	0.11 (0.91)	0.44 (0.09)	2.63	0.26 (0.29)	0.66 (0.71)	1.20
	550	0.17 (0.78)	0.73 (0.22)	1.68		0.71 (1.00)	1.34
	625	0.24 (0.70)	0.92 (0.30)	1.10		0.77 (1.00)	1.34

[a] τ_1 and τ_2 are lifetimes (ns), f_1 and f_2 are fractional intensities, and χ^2 is the reduced chi-square.

Table 2. Molecular Weights and Physical Properties of Polymers 1–3

polymer	molecular weight, $M_w \times 10^6$	polydispersity index, M_w/M_n	viscosity index, α	density, d [g/cm^3]	fractional free volume, FFV
1	4.2	2.5	1.03	0.96	0.16
2	7.5	1.8	0.79	0.99	0.17
3	5.2	3.2	0.80	0.91	0.26

we measured their fluorescence lifetimes with time-resolved fluorescence spectroscopy. For example, Figure 1 shows the time-resolved emission decay curve of **1**. Table 1 summarizes the fluorescence lifetimes of **1**–**3** in films and solutions. Two exponentials are required to adequately fit the observed decay dynamics in films. The emissions of **1** are characterized by a longer dominant fluorescence lifetime (τ_2) rather than a shorter one (τ_1). Longer emission wavelengths correlated with the longer lifetimes. The dominant lifetimes, τ_2, of **1** at 475, 550, and 625 nm were 1.18, 1.43, and 1.52 ns, respectively. This reflects a fluorescence relaxation time for energy migration from higher to lower energy levels. The lifetime is dependent on the fluorescence wavelength; this is unusual behavior, and it probably reflects that exciton diffusion is slow. In contrast with **1**, the emissions of **3** are characterized by a shorter dominant fluorescence lifetime (τ_1) rather than a longer one (τ_2). The dominant lifetimes, τ_1, of **3** at 475, 550, and 625 nm were 0.11, 0.17, and 0.24 ns, respectively. Namely, Table 1 shows another notable result: the longer the alkyl group in the side chain, the longer the lifetime. This can be explained by the idea that exciton deconfinement, along with Si−C rotational motion and intrachain exciton migration, is strongly restrained with an increase in the alkyl length of the alkylsilane moiety. This lifetime dependence on fluorescence wavelengths and alkyl side-chain length is also clearly shown in cyclohexane solutions. Actually, the values of the quantum yields were significantly dependent upon the alkyl length in the side chain. The fluorescence quantum yields of polymers **1**−**3** in cyclohexane were 53%, 38%, and 27%, respectively.

Table 2 describes several physical properties of **1**–**3**. As previously reported, **1** shows the stiff nature of the main chain, as determined by the high viscosity index ($\alpha = 1.03$ in THF at 40 °C).[4a] On the other hand, **2** and **3** have lower α values of 0.79 and 0.80, respectively. The α values of **1**–**3** are much higher than that of randomly coiled polystyrene ($\alpha = 0.69$). In general, a rodlike polymer has a high α value, within the range of $1.0 \leq \alpha \leq 1.7$, and a semiflexible polymer exhibits an α value in the range of $0.8 \leq \alpha \leq 1.0$, while a randomly coiled polymer shows an α value in the range of $0.5 \leq \alpha \leq 0.8$.[6] This means that the polymer chain of **1** is relatively rigid, and **2** and **3** are less rigid. Thus, **1** corresponds to a rodlike polymer, and **2** and **3** correspond to semiflexible polymers. This result indicates that the alkyl group length in the side chain significantly affects the main chain's stiffness. The reason for this can be explained as follows: the considerable stiffness of the main chain is a result of the strictly limited rotational freedom of bulky phenyl rings and intrachain van der Waals hydrophobic interactions between neighboring alkyl groups.

Fractional free volume (FFV) is correlated to a microvoid, or molecular scale gap, in a bulk solid film, which indicates the degree of intermolecular chain packing.[7] The FFV values of **1**–**3** were 0.16, 0.17, and 0.26, respectively, as estimated from their densities of 0.96, 0.99, and 0.91, respectively (Table 2).[8] Indeed, the FFV values of **1** and **2** were much lower than that of **3**. This indicates that the flexible long alkyl side chains behave like solvent molecules even in the solid state to effectively lower the molecular entropic energy by intermolecular packing.

According to Flory's theory, in order for a certain polymer to show lyotropic liquid crystallinity, the following conditions have to be satisfied.[9] First, the polymer concentration has to be higher than the critical concentration. Second, the polymer must have a high molecular weight sample. Third, the polymer chain must be a rigid-rod-like molecule. We have already reported that in a highly concentrated aromatic solvent such as toluene **1** has a lyotropic liquid crystalline nature due to the high molecular packing of its long *n*-alkyl chains and the stiffness of its main chain. Similarly, **2** and **3** in a highly concentrated toluene solution showed some characteristic birefringence textures under a polarizing optical microscope.

Figure 2 shows the WAXD patterns of **1**–**3** in cast films. Broad scattering signals are seen in a wide range from 15° to 30° due to the isotropic phase and/or $\pi-\pi$ stacking of phenyl rings in the side chain. As for **1**, a signal at a small angle of 4° is also seen. According to the Bragg equation, $\lambda = 2d \sin\theta$ ($\lambda = 1.54$ Å (Cu Kα)), the interlayer spacing, d, is calculated to be ∼22 Å.[4a] This is almost the same as the octadecyl length (22.5 Å), indicating a lamellar monolayer structure. For comparison with **1**, WAXD measurements were also conducted for **2** and **3,** which have an *n*-octyl group and a methyl group, respectively, in place of the *n*-octadecyl group. A sharp signal at the higher angle of 5.92° was clearly seen for **2**. d was calculated to be ∼14.9 Å, which is longer than the *n*-octyl length (10 Å), indicating an interdigitated bilayer structure. As for **3**, a sharp signal was clearly seen at the higher angle of 6.9°, with a corresponding d of ∼13 Å. This is much longer than the methyl length. The rotational freedom of the Si−C bond is relatively high, and the trimethylsilyl group takes a spherical shape. Thus, the interlayer spacing may be kept much greater than the methyl length. This result corresponds well to the high FFV value of **3**. The inset shows the 2D-WAXD patterns of **1–3** in the sheared films. In the sheared films, intense signals at smaller angles of diffraction appear on the equator, which is perpendicular to the shearing direction. This indicates that the smectic layer is parallel to the shearing direction.

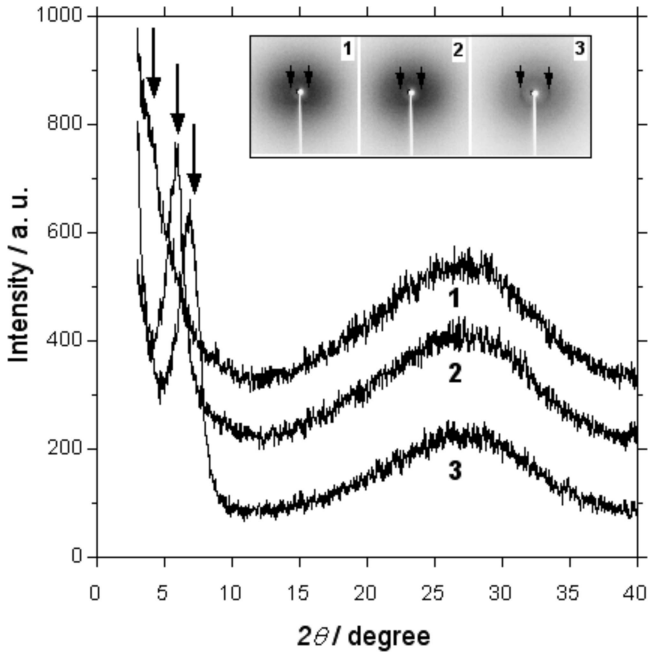

Figure 2. Wide-angle X-ray diffraction (WAXD) patterns of **1**–**3** in cast films (inset: two-dimensional (2D) WAXD patterns of the sheared films). The arrows indicate the signal peaks top in a small-angle region.

Figure 3 shows the polarized absorption spectra of **1**–**3** in sheared films as a function of the polarizer angle. The parallel and perpendicular components of the absorptions were significantly different from one another. As the angle of the polarizer to the shearing direction changed from 0 to 90° at intervals of 10°, the 430 nm absorption band due to the $\pi-\pi^*$ transition of the polymer backbone gradually decreased, while the 370 nm absorption band due to the $\pi-\pi^*$ transition of localized electrons in mesogenic repeat units increased.

The optical order parameter (S) is usually used to evaluate the degree of LC alignment. The S value is defined as $S = (D_{abs} - 1)/(D_{abs} + 2)$,[1a,4a,10] where D_{abs} is the apparent dichroic ratio of the absorption. If the molecular axes are ideally parallel and perpendicular to the shearing directions, the S values will be 1.0 and –0.5, respectively. For **1**, the D_{abs} at 430 nm was evaluated to be 5.56 from the polarized absorption spectra. Thus, the S value was calculated to be 0.60, which is closer to the ideal value of 1.0 than –0.5, confirming that the polymer main chain prefers to align in a direction parallel to the shearing direction. Compared to **1**, **2** and **3** showed much lower D_{abs} and S values (**2**: $D_{abs} = 2.4$, $S = 0.32$; **3**: $D_{abs} = 1.4$, $S = 0.11$). The longer alkyl group probably behaves like a solvent in a concentrated solution and thus is more effective at aligning the polymer chain parallel to the shearing direction than the shorter alkyl chains.

In summary, we clearly verified the effects of alkyl length on fluorescence quantum efficiency, main-chain stiffness, and optical order parameter of poly(diphenylacetylene)s containing alkylsilane moieties in their side chains. The longer alkyl groups in the side chains correlated with longer lifetimes. With an increase in the alkyl length, the intrinsic viscosity increases, leading to main-chain stiffness. A longer alkyl group is more effective at aligning the polymer chain parallel to the shearing direction than a shorter alkyl group. These results are expected to be helpful for molecular design of emissive conjugated polymers with high quantum yield and large optical anisotropy.

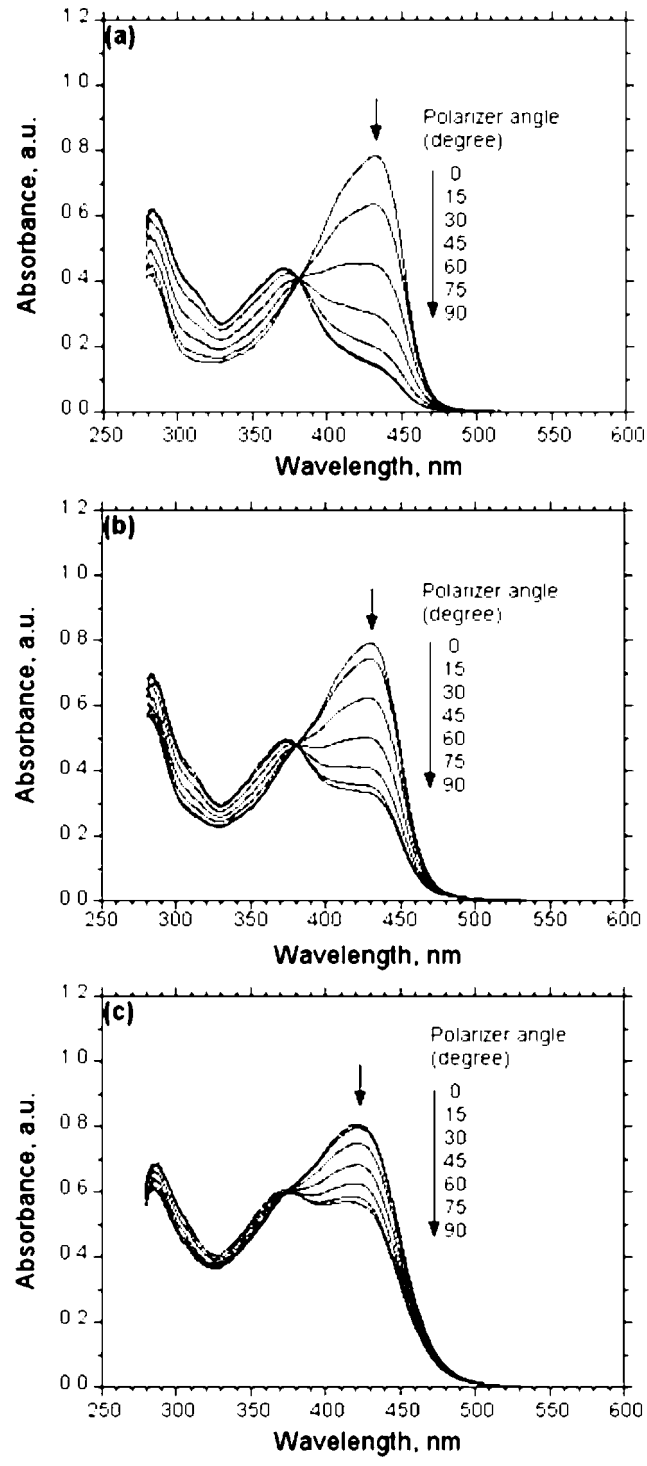

Figure 3. Polarized UV–vis absorption spectra of (a) **1**, (b) **2**, and (c) **3** in sheared films as a function of polarizer angle against shearing direction.

Acknowledgment. This research was supported by a Grant-in-Aid for Scientific Research in the priority area "Super-Hierarchical Structures" (No. 446) from the Ministry of Education, Culture, Sports, Science and Technology, Japan. M.F. is acknowledged in part for a grant from the Ministry of Education, Science, Sports, and Culture of Japan, for a Grant-in-Aid for Scientific Research, "Design, Synthesis, Novel Functionality of Nanocircle and Nanorod Conjugating Macromolecules (16205017)". This research was also supported by Kyungpook National University Research Fund, 2007. G.K. is acknowledged in part for a grant from the Korean Government (MOEHRD, Basic Research Promotion Fund) (KRF-2006-

003-D00144). The authors thank NOF Co., Ltd., Japan, for the donation of poly(1-phenyl-2-*p*-{trimethylsilylphenyl}acetylene) (**3**).

Supporting Information Available: Experimental methods; time-resolved emission decay curve of **1** in cyclohexane; UV–vis absorption and fluorescence spectra of **1**–**3** in cyclohexane. This material is available free of charge via the Internet at http://pubs.acs.org.

References and Notes

(1) (a) Ohira, A.; Swager, T. M. *Macromolecules* **2007**, *40*, 19–25. (b) Hayasaka, H.; Tamura, K.; Akagi, K. *Trans. Mater. Res. Soc. Jpn.* **2007**, *32*, 395–398. (c) Hayasaka, H.; Tamura, K.; Akagi, K. *J. Photopolym. Sci. Technol.* **2006**, *19*, 29–34. (d) Aldred, M.; Contoret, A. E. A.; Farrar, S.; Kelly, S. M.; Mathieson, D.; O'Neill, M.; Tsoi, W. C.; Vlachos, P. *Adv. Mater.* **2005**, *17*, 1368–1372. (e) Molenkamp, W.; Watanabe, M.; Miyata, H.; Tolbert, S. H. *J. Am. Chem. Soc.* **2004**, *126*, 4476–4477. (f) O'Neill, M.; Kelly, S. M. *Adv. Mater.* **2003**, *14*, 1135–1146. (g) Geng, Y.; Culligan, S. W.; Trajkovska, A.; Wallace, J. U.; Chen, S. H. *Chem. Mater.* **2003**, *15*, 542–549. (h) Moggio, I.; Le Moigne, J.; Arias-Marin, E.; Issautier, D.; Thierry, A.; Comoretto, D.; dellepiane, G.; Cuniberti, C. *Macromoelcules* **2001**, *34*, 7091–7099. (i) Grell, M.; Bradley, D. D. C. *Adv. Mater.* **1999**, *11*, 895–905. (j) Grell, M.; Knoll, W.; Lupo, D.; Meisel, A.; Miteva, T.; Neher, D.; Nothofer, H.-G.; Scherf, U.; Yasuda, A. *Adv. Mater.* **1999**, *11*, 671–675.

(2) (a) Hidayat, R.; Fujii, A.; Ozaki, M.; Teraguchi, M.; Masuda, T.; Yoshino, K. *Synth. Met.* **2001**, *119*, 597–598. (b) Fujii, A.; Hidayat, R.; Sonoda, T.; Fujisawa, T.; Ozaki, M.; Vardeny, Z. V.; Teraguchi, M.; Masuda, T.; Yoshino, K. *Synth. Met.* **2001**, *116*, 95–99. (c) Gontia, I.; Frolov, S. V.; Liess, M.; Vardeny, Z. V.; Ehrenfreund, E.; Tada, K.; Kajii, H.; Hidayat, R.; Fujii, A.; Yoshino, K.; Teraguchi, M.; Masuda, T. *Synth. Met.* **2001**, *116*, 91–94. (d) Shukla, A.; Ghosh, H.; Mazumdar, S. *Synth. Met.* **2001**, *116*, 87–90. (e) Hidayat, R.; Tatsuhara, S.; Kim, D. W.; Ozaki, M.; Yoshino, K.; Teraguchi, M.; Masuda, T. *Phys. Rev. B* **2000**, *61*, 10167–10173.

(3) (a) Lam, J. W.; Tang, B. Z. *Acc. Chem. Res.* **2005**, *38*, 745–754. (b) Lam, J. W. Y.; Tang, B. Z. *J. Polym. Sci., Part A: Polym. Chem.* **2003**, *41*, 2607–2629. (c) Shida, Y.; Sakaguchi, T.; Shiotsuki, M.; Sanda, F.; Freeman, B. D.; Masuda, T. *Macromolecules* **2005**, *38*, 4096–4102. (d) Sakaguchi, T.; Yumoto, K.; Shiotsuki, M.; Sanda, F.; Yoshikawa, M.; Masuda, T. *Macromolecules* **2005**, *38*, 2704–2709. (e) Sakaguchi, T.; Shiotsuki, M.; Masuda, T. *Macromolecules* **2004**, *37*, 4104–4108. (f) Teraguchi, M.; Suzuki, J.; Kaneko, T.; Aoki, T.; Masuda, T. *Macromolecules* **2003**, *36*, 9694–9697. (g) Teraguchi, M.; Masuda, T. *Macromolecules* **2002**, *35*, 1149–1151. (h) Aoki, T.; Kobayashi, Y.; Kaneko, T.; Oikawa, E.; Yamamura, Y.; Fujita, Y.; Teraguchi, M.; Nomura, R.; Masuda, T. *Macromolecules* **1999**, *32*, 79–85. (i) Teraguchi, M.; Masuda, T. *J. Polym. Sci., Part A: Polym. Chem.* **1998**, *36*, 2721–2725. (j) Tsuchihara, K.; Masuda, T.; Higashimura, T. *Macromolecules* **1992**, *25*, 5816–5820. (k) Tsuchihara, K.; Masuda, T.; Higashimura, T. *J. Am. Chem. Soc.* **1991**, *113*, 8548–8549.

(4) (a) Kwak, G.; Minakuchi, M.; Sakaguchi, T.; Masuda, T.; Fujiki, M. *Chem. Mater.* **2007**, *19*, 3654–3661. (b) Kwak, G.; Fukao, S.; Fujiki, M.; Sakaguchi, T.; Masuda, T. *Chem. Mater.* **2006**, *18*, 5537–5542.

(5) (a) Kulkarni, A. P.; Kong, X.; Jenekhe, S. A. *Macromolecules* **2006**, *39*, 8699–8711. (b) Kulkarni, A. P.; Wu, P.-T.; Kwon, T. W.; Jenekhe, S. A. *J. Phys. Chem. B* **2005**, *109*, 19584–19594. (c) Jenekhe, S. A.; Lu, L.; Alam, M. M. *Macromolecules* **2001**, *34*, 7315–7324, and references therein.

(6) (a) Sato, T.; Terao, K.; Teramoto, A.; Fujiki, M. *Polymer* **2003**, *44*, 5477–5495. (b) Nakahima, H.; Fujiki, M. *Macromolecules* **2001**, *34*, 7558–7564. (c) Morese, D. C. *Macromolecules* **1998**, *31*, 7044–7067.

(7) Toy, L. G.; Nagai, K.; Freeman, B. D.; Pinnau, I.; He, Z.; Masuda, T.; Teraguchi, M.; Yampolskii, Y. P. *Macromolecules* **2000**, *33*, 2516–2524.

(8) (a) van Krevelen, D. W. *Properties of Polymers: Their Correlation with Chemical Structure; Their Numerical Estimation and Prediction from Additive Group Contributions*, 3rd ed.; Elsevier Science: Amsterdam, 1990; pp 71–107. (b) Bondi, A. *Physical Properties of Molecular Crystals, Liquids, and Glasses*; John Wiley and Sons: New York, 1968; pp 25–52, 53–97.

(9) (a) Flory, P. J. *Proc. R. Soc. London* **1956**, *A234*, 73. (b) Flory, P. J. *Adv. Polym. Sci.* **1984**, *59*, 1.

(10) Kawatsuki, N.; Tachibana, T.; An, M.-X.; Kato, K. *Macromolecules* **2005**, *38*, 3903–3908.

MA702592U